OPEN

Statin-induced myopathic changes in primary human muscle cells and reversal by a prostaglandin F2 alpha analogue

Stefanie Anke Grunwald [1,2*], Oliver Popp[3,4], Stefanie Haafke[1,2], Nicole Jedraszczak[1,2], Ulrike Grieben[1,2], Kathrin Saar [6], Giannino Patone[6], Wolfram Kress[7], Elisabeth Steinhagen-Thiessen[5], Gunnar Dittmar [3,4] & Simone Spuler [1,2*]

Statin-related muscle side effects are a constant healthcare problem since patient compliance is dependent on side effects. Statins reduce plasma cholesterol levels and can prevent secondary cardiovascular diseases. Although statin-induced muscle damage has been studied, preventive or curative therapies are yet to be reported. We exposed primary human muscle cell populations (n = 22) to a lipophilic (simvastatin) and a hydrophilic (rosuvastatin) statin and analyzed their expressome. Data and pathway analyses included GOrilla, Reactome and DAVID. We measured mevalonate intracellularly and analyzed eicosanoid profiles secreted by human muscle cells. Functional assays included proliferation and differentiation quantification. More than 1800 transcripts and 900 proteins were differentially expressed after exposure to statins. Simvastatin had a stronger effect on the expressome than rosuvastatin, but both statins influenced cholesterol biosynthesis, fatty acid metabolism, eicosanoid synthesis, proliferation, and differentiation of human muscle cells. Cultured human muscle cells secreted ω-3 and ω-6 derived eicosanoids and prostaglandins. The ω-6 derived metabolites were found at higher levels secreted from simvastatin-treated primary human muscle cells. Eicosanoids rescued muscle cell differentiation. Our data suggest a new aspect on the role of skeletal muscle in cholesterol metabolism. For clinical practice, the addition of omega-n fatty acids might be suitable to prevent or treat statin-myopathy.

Patient non-compliance to medication due to side effects is a major healthcare concern. Statin side effects on skeletal muscle causes about 70% of patients to discontinue treatment[1–7]. Millions of patients ingest statins to reduce blood cholesterol levels thereby preventing cardiovascular diseases. Most statin-intolerant patients experience muscle cramps and myalgia, with occasional asymptomatic elevation of creatine kinase and weakness. Although skeletal muscle damage has been studied in mice[8], it is unknown whether the same or different mechanisms underlie the various myopathic phenotypes and how we can circumvent or treat statin-induced changes in skeletal muscle. Also, the effect of lipophilic and/or hydrophilic statins on muscle is unclear. Removal of cholesterol might affect membrane structure and lipid rafts that are essential for signalling and cellular compartmentalization. Given that, cholesterol-lowering agents including proprotein convertase subtilisin/kexin type 9 –inhibitors (PCSK9-inhibitors), would lead to the same spectrum of muscle complaints which has not been reported yet[9]. Alternatively, statins might influence pathways downstream of the hydroxymethylglutaryl-coenzyme A

[1]Muscle Research Unit, Experimental and Clinical Research Center, a joint cooperation between the Charité Universitätsmedizin and the Max Delbrück Center for Molecular Medicine, Berlin, 13125, Germany. [2]Charité Universitätsmedizin Berlin, Berlin, 13125, Germany. [3]Mass Spectrometry Core Facility, Max Delbrück Center for Molecular Medicine in the Helmholtz Society, Berlin, 13125, Germany. [4]Mass Spectrometry Facility, Berlin Institute of Health, Berlin, 13125, Germany. [5]Interdisciplinary Lipid Metabolic Center, Charité Universitätsmedizin Berlin, Berlin, 13353, Germany. [6]Genetics and Genomics of Cardiovascular Diseases, Max Delbrück Center for Molecular Medicine in the Helmholtz Society, Berlin, 13125, Germany. [7]Institute for Human Genetics, Julius-Maximilians-University of Würzburg, Würzburg, 97074, Germany. *email: stefanie.grunwald@charite.de; simone.spuler@charite.de

(HMG-CoA) reduction into mevalonate by 3-hydroxy-3-methylglutaryl-CoA reductase (HMGCR) that is inhibited by statins and causing a distinct myopathy[10,11].

Mevalonate can be metabolized into squalene for cholesterol biosynthesis[12] or into metabolites, i.e. farnesyl-pyrophosphate and geranylgeranyl-pyrophosphate, involved in isoprenoid synthesis, protein prenylation, and ubiquinone synthesis. Consequently, hypotheses for statin-related side effects include a decrease in ubiquinone synthesis, cholesterol, and vitamin D levels, and a loss of isoprenoid metabolites. Altering vitamin D levels and protein ubiquination remain an intriguing yet controversial hypothesis for causing statin-induced side effects[11,13–16]. Interventions into isoprenoid synthesis have been associated with ATP depletion and DNA damage and therefore suggested for cancer therapy[17,18]. Since ubiquinone is critical for the mitochondrial respiratory chain, mitochondrial impairment has been reported *in vitro* as well as in statin-treated patients[19]. Ubiquinone supplementation is argumentatively beneficial to patients[20]. However, most studies have been performed in non-human muscle or human non-muscle cell lines or animals and only focus on mevalonate depletion.

In this study, we asked whether there are key signalling pathways in muscle that are significantly interfered by statins and may have a statin myopathy management potential. We chose an integrated approach to study the effects of a lipophilic and a hydrophilic statin in many individual primary human myoblast cells at molecular, cellular, and functional levels[21]. We developed a new assay for mevalonate detection and showed that statins have a significant effect on gene and protein expression profiles. Our model for signal transduction pathway suggests statin-induced metabolic changes upstream of mevalonate, particularly in mitochondrial ß-oxidation and eicosanoid synthesis. Eicosanoids have profound effects on inflammation, cell proliferation and differentiation, and acts as pain mediators. Primary human muscle cells secrete eicosanoids and prostaglandins *in vitro*. Arachidonic acid derived eicosanoid levels changed time dependently. Furthermore, statins directly influence the proliferative and regenerative features of skeletal muscle cells. Eicosanoid-species substitution to simvastatin-treated primary human muscle cells rescue these effects. Statin myopathy, therefore, appears as a distinct and potentially treatable myopathy driven by HMG-CoA accumulation rather than mevalonate depletion.

Results

In primary human muscle cell populations obtained from 22 patients we investigated key signalling pathways that are significantly interfered by statins in muscle cells and their impact on cellular and molecular levels.

Simvastatin more than rosuvastatin extensively alters myotube expressome. Transcriptome data obtained from statin-treated primary human myotubes group clearly separate from untreated and DMSO-treated samples on a PCA analysis plot (Fig. 1A). A concern about studying primary human samples derived from individuals of different age and gender usually has been the potentially high variation between samples. Clinical patient information is provided in Supplementary Table S1. Here, however, we can show that primary human samples behave very similar among various conditions but different for both statins (Fig. 1A). We found that simvastatin had a dramatic effect on primary human muscle cells, much more than rosuvastatin. 1807 genes (FDR < 0.05) were differentially expressed after exposure to simvastatin (Fig. 1B, Supplementary Table S2, Supplementary Dataset File 1). Simvastatin had a particularly strong impact on RNA metabolism (Table 1). The number of genes affected by rosuvastatin was only 68 (FDR < 0.05) (Supplementary Table S3, Supplementary Dataset File 2) with a main impact on lipid and cholesterol metabolism.

When transcriptome and proteome of identical samples are compared, there may or may not be a good overlap. We found that on proteome level 3255 skeletal muscle proteins were significantly identified after exposure to statins (Supplementary Fig. S1, Supplementary Dataset File 3; Supplementary Tables S5, S6). Proteins belonging to lipid metabolic, small molecule metabolic, and cellular, developmental as well as RNA metabolic processes were particularly affected (Supplementary Dataset File 4). A Venn diagram (Fig. 1C) demonstrates that 19% of genes and proteins in simvastatin and 6% in rosuvastatin treated myotubes were significantly differentially expressed at proteome <u>and</u> transcriptome levels when compared to controls. Five gene products are differently regulated by both statins at mRNA as well as protein levels: Calsyntenin-2 (CLSTN2), lanosterol 14-alpha demethylase (CYP51A1), squalene synthase (FDFT1), isopentenyl-diphosphate delta-isomerase 1 (IDI1), and tubulin beta-2B chain (TUBB2B) (Supplementary Table S7). All five are involved in cell adhesion and cholesterol biosynthesis. The degree of similarity between RNA-Seq and proteome-data is visualized in a circus plot (Supplementary Video)[22].

The significant effect of statins on the transcriptome and proteome of primary human muscle cells was unexpected and widespread. Because both, simvastatin and rosuvastatin, induce "statin-myopathy" we focussed our further analysis on pathways in muscle cells that were influenced by both statins. These were fatty acid metabolism, fatty acid import, and lipid metabolic processes (Table 1, Supplementary Dataset File 4).

Muscle cells possess a similar repertoire for cholesterol biosynthesis as liver. We next asked how the muscle was equipped to synthesize and metabolize cholesterol. We found key enzymes for cholesterol biosynthesis (hydroxymethylglutaryl-Coenzym A-synthase HMGCS1, HMGCR, CYP51A1, 7-dehydrocholesterol reductase DHCR7) as well as cholesterol transport (low density lipoprotein receptor LDLR, ATP-binding cassette transporter ABCA1 and ABCG1) expressed in human muscle cells and significantly altered by different exposure to statins. We further analysed the transcript variants of HMGCR of human muscle cells and compared them to human liver (HepG2 cells) (Fig. 2A). HMGCR transcript variants (ENST00000287936 and ENST00000343975 that excludes exon 13) have an impact on cholesterol metabolism regulation and statin efficacy[23]. The transcripts in primary human myotubes and HepG2 cells were identical (Fig. 2A). In our OMICs data set (Supplementary Table S4) the ENST00000343975 was also detectable at low levels. We then tested to what extent statins added to primary human muscle cells would influence cholesterol and mevalonate levels, or expression of cholesterol dependent gene expression (Fig. 2B–D). To accomplish this, we redeveloped a simple assay for mevalonate
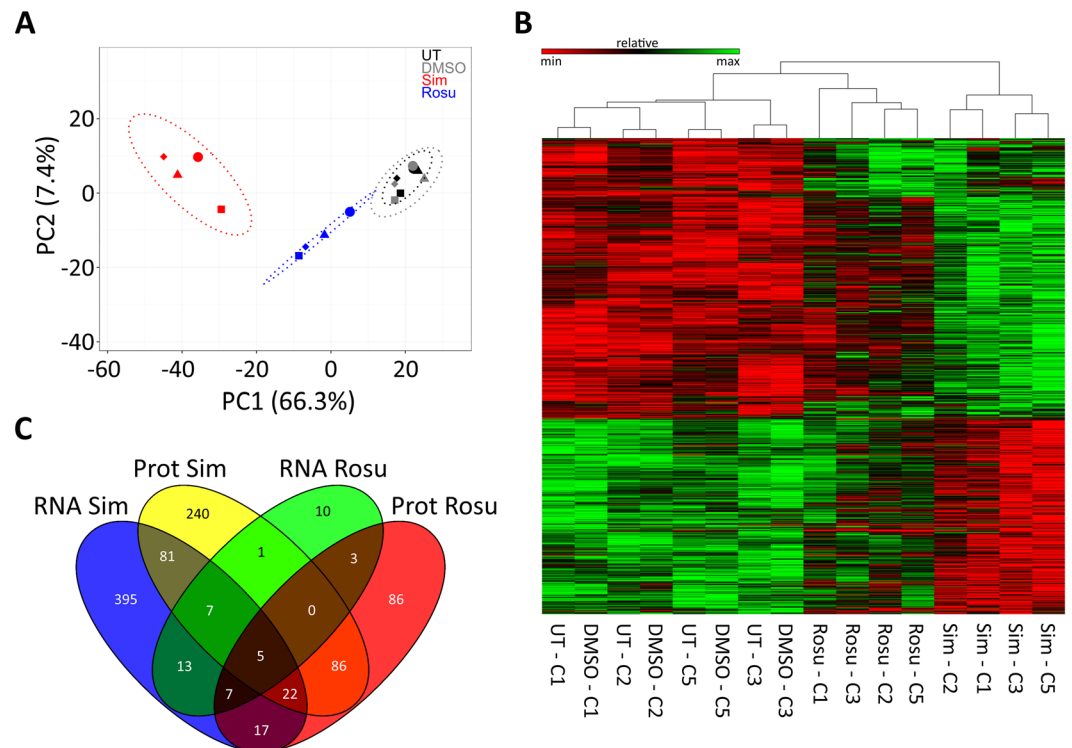
Figure 1. Gene expression profiling of primary human myotubes exposed to statins. Four primary human myotube cell populations from four different statin naïve donors were left untreated (UT), treated with DMSO, rosuvastatin (Rosu) or simvastatin (Sim). (**A**) Principal components analysis (PCA) of RNA-Seq samples. The PCA plot shows a clear grouping. (**B**) Heatmap of RNA-Seq samples represents log2 transformed normalized count data of differently expressed genes. Samples of each statin group cluster hierarchically together. Untreated and DMSO treated samples are equally clustered confirming that DMSO has no significant effect on RNA expression data. (**C**) Venn diagram displaying overlaps between proteome and transcriptome expression data from simvastatin and rosuvastatin groups. Cell populations C1-C3; C5 used in this experiment, see Supplementary Table S1. See also Supplementary Fig. S1 and Supplementary Dataset Files 1 and 2.

determination in human muscle cells. Cholesterol and mevalonate levels in primary human myotubes were significantly lowered by statins in a concentration dependent manner. (Fig. 2B,C). On mRNA level as assessed by qPCR, we found that statins increased HMGCS and HMGCR (Fig. 2D), the same effects that have been described for liver including LDL receptor[24]. Eight protein coding transcript variants are known for LDLR. In our RNASeq data set, we found six of them differentially expressed (between statin and controls) with similar fold changes (see Supplementary Table S4). ENST00000558518, ENST00000558013, ENST00000535915, and ENST00000545707 are the most supported transcript variants throughout databases. In our data set, ENST00000545707 (682 amino acids) had the highest number of uniquely mapped and total transcript reads (FPKM 7.8–19.4). This variant misses LDL receptor class A3-5 and the EGF-like 3 domain that are linked to familiar hypercholesterolemia, i.e. rs121908028, rs121908029, rs28942083, rs748944640 (UniProt identifier P01130-2). LDLR binding partner PCSK9 has only one protein coding transcript variant which is 2fold upregulated in rosuvastatin-treated primary human myotubes. Our data show, that primary human myotubes possess the same repertoire for cholesterol biosynthesis and expression regulation feedback mechanisms as liver cells, an important condition for our further analyses.

Statins interfere with fatty acid metabolism. To further analyze pathways significantly affected by both statins, we used Gene Ontology enRIchment anaLysis (GOrilla) and the Database for Annotation, Visualization and Integrated Discovery (DAVID) analysis (Supplementary Dataset File 4). Within the gene ontology terms *fatty acid metabolism, fatty acid import, and lipid metabolic processes*, we identified significant effects on genes involved in lipid, fatty acid, and arachidonic/eicosanoid metabolism as well as on retinoic acid response of the retinoid X receptor's (RXR) pathway and carnitine shuttling (Fig. 3A). Carnitine palmitoyltransferase I (CPT1) was up to 12-fold upregulated at protein level. Based on these findings, we qualitatively analysed gene and protein interactions known or predicted to HMGCR and included the quantitative abstraction level for pathway modelling. We modelled a regulatory network showing the statin-induced alterations on HMGCR-associated pathways in human muscle. (Fig. 3B, Supplementary Table S8). Among the general impact of statins on acetyl-CoA dependent metabolic processes we found particularly interesting upregulation of fatty acid desaturases and elongases. Both, fatty acid desaturases and elongases catalyse precursor molecules for prostaglandin and eicosanoid

Expression level	GO Term – Top 10	P-value
Simvastatin Transcriptome	• SRP-dependent cotranslational protein targeting to membrane	5.65 E-29
	• Cotranslational protein targeting to membrane	1.60 E-28
	• Protein targeting to ER	1.27 E-26
	• rRNA processing	5.10 E-26
	• Establishment of protein localization to endoplasmic reticulum	7.75 E-26
	• rRNA metabolic process	3.00 E-24
	• Protein localization to endoplasmic reticulum	4.42 E-24
	• Translational initiation	1.88 E-23
	• Nuclear-transcribed mRNA catabolic process, nonsense-mediated decay	8.48 E-23
	• Viral transcription	1.03 E-21
Simvastatin Proteome	• Negative regulation of cellular process	2.30E-04
	• Regulation of biological quality	3.91 E-04
	• Signal transduction	2.69 E-05
	• RNA metabolic process	7.27 E-04
	• Small molecule metabolic process	5.35 E-04
	• Regulation of localization	2.37 E-04
	• Immune system process	4.85 E-04
	• Macromolecule biosynthetic process	8.40 E-04
	• Multicellular organismal process	2.72 E-04
	• Positive regulation of response to stimulus	8.05 E-04
Rosuvastatin Transcriptome	• Secondary alcohol biosynthetic process	3.29 E-31
	• Sterol biosynthetic process	5.28 E-30
	• Cholesterol biosynthetic process	1.47 E-29
	• Secondary alcohol metabolic process	9.54 E-27
	• Cholesterol metabolic process	6.92 E-26
	• Sterol metabolic process	1.47 E-25
	• Alcohol biosynthetic process	9.80 E-25
	• Steroid biosynthetic process	4.95 E-23
	• Organic hydroxy compound biosynthetic process	7.60 E-22
	• Regulation of cholesterol biosynthetic process	1.21 E-21
Rosuvastatin Proteome	• Small molecule metabolic process	1.73 E-04
	• Oxidation-reduction process	7.32 E-05
	• Small molecule catabolic process	6.13 E-04
	• Cellular lipid metabolic process	9.49 E-07
	• Monocarboxylic acid metabolic process	9.03E-06
	• Small molecule biosynthetic process	1.26 E-05
	• Lipid metabolic process	3.11 E-09
	• Regulation of lipid metabolic process	7.54 E-05
	• Lipid biosynthetic process	2.90 E-08
	• Organic hydroxy compound metabolic process	6.49 E-08
Common GO-terms at transcriptome and proteome level influenced by both statins	Lipid metabolic process	8.07 E-11
	• Cholesterol metabolic process	5.65 E-10
	• Sterol metabolic process	1.65 E-09
	• Cholesterol biosynthetic process	1.37 E-08
	• Isoprenoid biosynthetic process	1.15 E-06
	• Triglyceride metabolic process	1.67 E-04
	• Fatty acid metabolic process	8.52 E-05
	• Arachidonic metabolism	3.33 E-04

Table 1. Biological process clustering. Genes and proteins differentially expressed in statin-treated primary human myotubes at mRNA and protein level were clustered into biological processes using GOrilla. The GO Term Top10 are different for each statin but similar at both expression levels. Lipid and cellular metabolic processes are most commonly modified by both statins at both expression levels. The p-values correspond to number of genes/proteins clustered into a GO node. (Supplementary Tables S2–S6).

synthesis, molecules involved in inflammation, mitochondrial function, and mediating pain; a common finding in statin-induced myopathy. We propose that the statin effect in muscle may be driven by HMG-CoA and acetyl-CoA accumulation rather than a loss of mevalonate downstream metabolites.
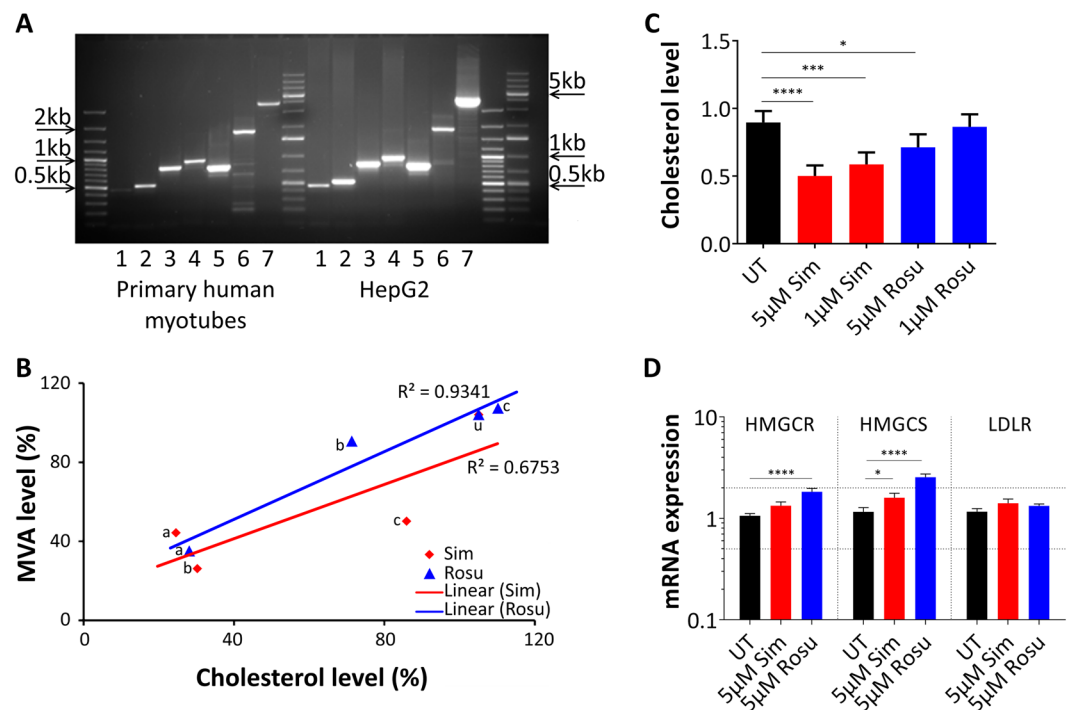
Figure 2. Statin effect in primary human myotubes on mevalonate and cholesterol dependent gene expression level. (**A**) HMGCR transcript variants amplified for exon 1–20 in primary human myotubes (cell population C11) and liver HepG2 cells. Primary human muscle cells and HepG2 cells share the identical HMGCR transcripts. Unspecific bands in lane 6 were sequenced. [1, Exon1–5; 2, Exon 3-8; 3, Exon 6–11; 4, Exon 9-14; 5, Exon 12-17; 6, Exon 15-20; 7, Exon 1-20; full-length gel was cropped without losing any relevant information, original picture scan in Supplementary Fig. S7] (**B**) Mevalonate levels in primary human myoblasts after 72 h statin treatment at different concentrations in delipidated medium. Mevalonate levels correlate to cholesterol levels. Data were normalized to total protein level and relativized to DMSO treated samples. (n = 4; cell populations C1, C9, C11, C16) (**C**) Relative cholesterol levels were determined under delipidated medium conditions in primary human myoblasts after 72 h statin treatment at different concentrations. (error/bars represent mean with SD; n = 3; cell populations C4, C9, C17) (**D**) Relative mRNA expression of HMGCR, HMGCS, and LDLR were examined in primary human myoblasts undergoing differentiation under statin treatment (5 µM) for 72 h-96 h. The results were normalized to two reference genes and calculated relatively to DMSO-treated samples. (error/bars represent mean with SEM; n = 6; cell populations C2-C4, C11-C13). For cell populations used see Supplementary Table S1. [UT, untreated (black); Sim, simvastatin (red); Rosu, rosuvastatin (blue); a = 50 µM, b = 5 µM, c = 1 µM; HMGCR, 3-hydroxy-3-methylglutaryl-CoA reductase; HMGCS, 3-hydroxy-3-methylglutaryl-CoA synthase 1; LDLR, low density lipoprotein receptor].

Indeed, we found that a number of genes involved in eicosanoid synthesis, such as the ATP-binding cassette sub-family D member 1 (ABCD1), the elongation of very long chain fatty acids 4 and 6 (ELOVL4,6) as well as the aldo-keto reductase family 1 member D1 (AKR1D1), fatty acid desaturase (FADS), phospholipase A2 group III (PLA2G3), and prostaglandin-endoperoxide synthase 1 (PTGS1) were significantly different expressed (Fig. 3A,B). PTGS1 is constitutively expressed in a wide range of tissues and PTGS2 is the inducible isoform. Significant reduction of PTGS1 (Fig. 3C), but not PTGS2, the key enzyme in ω-3 and ω-6 fatty acid metabolism converting eicosapentaenoic acid and arachidonic acid to eicosanoids including prostaglandins, points a disturbance in eicosanoid biosynthesis.

Eicosanoid AL-8810 reverses the effect off simvastatin on primary human muscle cells. If an impairment in eicosanoid biosynthesis would be responsible for statin related side effects on muscle, reconstitution with eicosanoids might be beneficial. We first identified parameters on cellular level that would be possible to quantify and measured the effect of statins on proliferation and differentiation in primary human muscle cells. Myoblast proliferation decreased in response to both, simvastatin and rosuvastatin, in a concentration-dependent manner (Fig. 4A, Supplementary Fig. S2B). We found no evidence for significant statin toxicity (Supplementary Fig. S2A) or oxidative stress as measured by nitric oxide concentration (Supplementary Fig. S3A,B). Rescue experiments with mevalonate and geranylgeranyl pyrophosphate demonstrate that the effect on proliferation was indeed statin specific (Supplementary Fig. S2B). In addition, simvastatin markedly delayed primary human myoblast differentiation as quantified by fusion index, and by myosin heavy chain expression on mRNA and protein level (Fig. 4B,C).
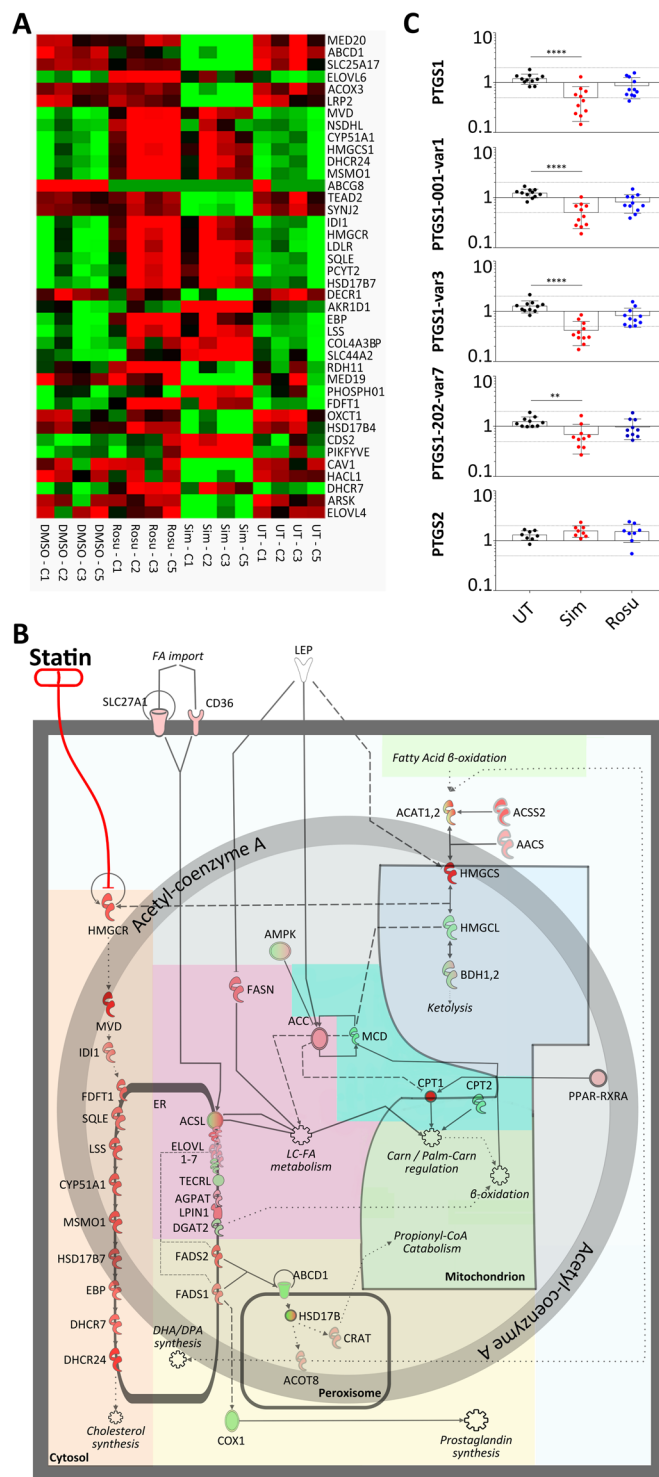
Figure 3. Statin influence on lipid metabolic processes and on PTGS1 mRNA expression in primary human myotubes. (**A**) RNA expression of primary human myotubes treated with statins compared to controls. Heatmap displays gene enrichment in lipid metabolic processes at RNA level. (Green – downregulated; Red – upregulated; n = 4; cell populations C1-C3; C5) (**B**) Signalling pathway model of statin-induced alterations in muscle lipid metabolism. Statin-induced changes in cholesterol biosynthesis (orange) are a direct effect of HMGCR inhibition. This also affects HMG-CoA synthesis and ketone body metabolism (blue) and especially Ac-CoA. Ac-CoA directly affects fatty acyl and triglyceride biosynthesis (magenta) and impairs eicosanoid synthesis (yellow). Also, Ac-CoA influences carnitine-palmitoyl transferases (turquois) and mitochondrial beta oxidation (green). See also Supplementary Table S8 for expression values and gene names. (**C**) Transcript variant expression study of PTGS1 and PTGS2 in primary human myotubes statin-treated for 96 h. For PTGS1, we analysed three different variants. PTGS1 variant 3 shows the lowest expression values (mean fold change = 0.41). Thus, it mainly reflects the low expression level detected for all variants. (error/bars represent

mean with SD; n = 11; ****p < 0.0001; cell populations C1-C3, C5, C6, C10, S3–S6) See Supplementary Table S9 for PCR primer details. For cell populations used see Supplementary Table S1. [UT, untreated (black); Sim, 5 μM simvastatin (red); Rosu, 5 μM rosuvastatin (blue); Ac-CoA, acetyl coenzyme A; HMG-CoA, 3-hydroxy-3-methylglutaryl coenzyme A; HMGCR, 3-hydroxy-3-methylglutaryl-CoA reductase; PTGS, prostaglandin-endoperoxide synthase].

In a time-series experiment, we analysed eicosanoid profile changes in the supernatant from statin-treated primary human myoblasts under fusion conditions compared to DMSO control. Because we found primary human myoblast fusion under statin treatment still occurring but delayed, we analysed the first 6 h to 36 h of myoblast fusion onset as well as 96 h matching the expressome analysis time point. (Supplementary Fig. S4, Supplementary Table S10) Long-chain ω-6 polyunsaturated fatty acids (PUFA) arachidonic acid derived eicosanoids (PGF2a, 8-iso-PGF2a, PGD2, LXB4, LXA4) showed increased levels in the supernatant from simvastatin-treated primary human myoblasts compared to DMSO control. At 96 h, the pro-inflammatory PGD2, PGF2a and 8-iso-PGF2a levels in simvastatin decreased again matching low PTGS1 mRNA expression levels after 96 h whereas the inflammatory resolving LXA4 continued to increase. LXB4 was detected only from 6 h to 36 h. Long-chain ω-3 eicosapentaenoic acid derived PGE3 and the PUFA 13-HODE were completely absent in simvastatin-treated primary human myoblasts at any time point. PGE3 showed higher levels after rosuvastatin treatment compared to controls after 96 h. Inflammatory resolving ω-3 docosahexaenoic acid derived eicosanoid RvD2 levels were only detectable in the supernatant from simvastatin-treated primary human myoblasts and dropped down to zero at 96 h. This suggests that long-chain ω-6 PUFA metabolites were affected in simvastatin-treated primary human muscle cells.

We then tested six different eicosanoid species at concentrations reported in the literature (Supplementary Table S11) for their effect on proliferation and differentiation of primary human muscle cells during statin exposure. In these experiments, we used primary human muscle cell populations obtained from statin naïve and statin-experienced patients. No significant differences were found for treating muscle cell populations from statin naïve and statin-experienced patients *in vitro* with eicosanoids and statins. We identified AL-8810, an 11β-fluoro receptor analog of prostaglandin 2α, but not prostaglandin 2α, to significantly reverse the effect of simvastatin on proliferation and differentiation (Fig. 4C,D). AL-8810 had no effect on rosuvastatin treated myotubes (Supplementary Fig. S5A–C). 5,6-EET, another arachidonic acid metabolite, increased proliferation independently from the statin effect (8Z,14Z). EDA, found in human milk, showed a negative trend on proliferation without impact on myotube fusion. Other eicosanoids, such as 12-HETE, did not have a significant effect on statin-treated primary human muscle cells.

Thus, eicosanoid species from arachidonic acid influence primary human muscle cell proliferation and fusion. For simvastatin, eicosanoids have potential to ameliorate statin-induced changes in primary human myotubes.

Discussion

In our comprehensive expressome analysis and molecular and cellular assessment of muscle related statin effects we discovered that statins have profound and unexpected effects on the transcriptome and proteome of primary human muscle cells. Some cellular functions such as RNA synthesis and turnover were much more influenced by the lipophilic simvastatin than by the hydrophilic rosuvastatin, but cholesterol and fatty acid metabolism, mitochondrial metabolism as well as eicosanoid synthesis pathways were severely affected irrespective of the class of statin that was delivered. The phenotype could be rescued by the addition of eicosanoids.

We were surprised to find a dramatic effect of statins on cholesterol and eicosanoid synthesis in primary human muscle cells. We investigated the cellular gene set to synthesise cholesterol and found that muscle and liver cells (HepG2) share the same repertoire for cholesterol biosynthesis (i.e. HMGCS1, HMGCR, CYP51A1, DHCR7) and transport (i.e. ABCA1, ABCG1, LDLR). Besides Scavenger Receptor Class B Member SCARB1, cholesterol biosynthesis proteins have been positively detected in human skeletal muscle (https://www.protein-atlas.org). It possibly points towards a so far underestimated role of skeletal muscle for their own cholesterol homeostasis[25]. Our data provide evidence that muscle contributes markedly to cholesterol synthesis. The human body consists of more than 25% muscle mass, whereas the liver only makes up 2–3%. If cholesterol synthesis is an integral part of muscle function, it would be interesting to speculate whether muscular cholesterol is also secreted into the blood circulation or whether skeletal muscle only produces cholesterol for its own needs. It will be the role of future experiments employing *in vivo* microdialysis[26] together with metabolomic plus lipidomic analysis that will provide the necessary answers.

Genes involved in cholesterol metabolism like HMGCR, HMGCS1, LDLR, and PCSK9 are increased under statin treatment in primary human muscle cells[27]. If HMG-CoA synthesis is increased but its reduction inhibited by statins, HMG-CoA levels increase and accumulate[28]. Therefore, HMG-CoA might reconvert into ketone metabolites, namely acetoacetyl-CoA and Ac-CoA. Acetoacetyl-CoA synthetase and Ac-CoA acetyltransferase expression are increased suggesting ketolysis or Ac-CoA formation. Muscle is not known to be able to produce ketone bodies whereas liver would be. In rat hepatocytes, high Ac-CoA concentrations trigger insulin resistance *in vivo*[29]. Excess Ac-CoA has been also observed in diabetes patients as insulin negatively regulates gluconeogenese by suppressing Ac-CoA. Indeed, clinical observations associate statins with an increased risk for diabetes mellitus type-2[30–32]. Ac-CoA is a central metabolite. Multiple metabolic effects are possible and are intermingled between each other. Increased Ac-CoA would shuttle into the tricarboxylic acid cycle, carnitine-palmitoyl-transferases (CPT1) as well as fatty acid and triglyceride biosynthesis (Fig. 3A,B). All pathways appear affected by statins in muscle as we find increased protein levels of Ac-CoA carboxylase alpha, a very prominent upregulation of CPT1, and an influence on key enzymes for fatty acid synthesis and mitochondrial ß-oxidation (Supplementary Table S8, Fig. 3A,B). On the one hand, Ac-CoA carboxylase alpha, an ACC family member, converts Ac-CoA
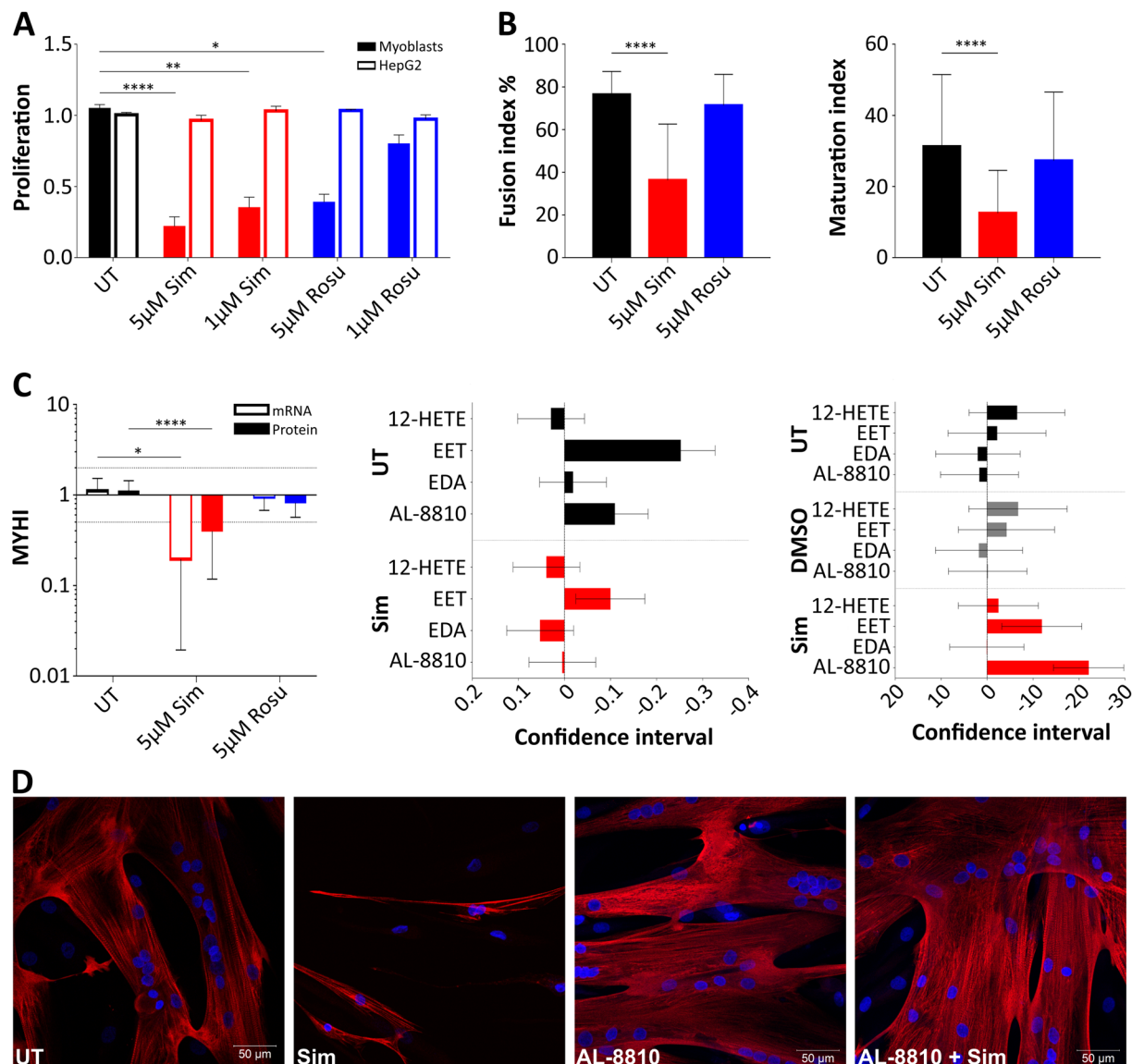
Figure 4. Statin influence on fatty acid metabolism of primary human myotubes. (**A**) Cell proliferation (BrdU) test: Primary human myoblasts and liver HepG2 cells were treated with statins for 72 h. At 5 µM concentration, statins negatively influence primary human myoblast but not HepG2 proliferation. The proliferation data were relatively calculated to DMSO-treated samples to quench the effect of DMSO. (error/bars represent mean with SEM; n = 8 for myoblasts; cell populations C4, C9, C11-C15, C17, C18; n = 4 for HepG2) (**B**) Differentiation of primary human myoblasts under statin treatment for 96 h. Primary human myoblast differentiation into myotubes is delayed under treatment with 5 µM simvastatin or 5 µM rosuvastatin. Myotube fusion and maturation index (number of nuclei per myotube) were determined by counting MYHI (red) positively immunolabelled myotubes and HOECHST (blue) stained nuclei using the cell image analysis software CellProfiler v.2.1.1. (error/ bars represent mean with SD; n = 8, 2-4 immunofluorescent pictures counted each, cell populations C5, C6, C10, C13, S2, S4–S6). (**C, left**) MYHI mRNA and protein expression were examined in primary human myotubes treated with 5 µM statin for 84 h to 96 h under differentiation condition relative to DMSO-treated samples. Dashed lines represent 2 fold and 0.5 fold expression changes. (error/bars represent mean with SD; n = 4). (**C, middle**) Proliferation of primary human myoblasts under simvastatin and/or eicosanoid species treatment relative to DMSO. (5)6-EET ameliorates proliferation for simvastatin-treated samples. (95% confidence interval; right side – positive effect, left side – negative effect; n = 8, cell populations C5, C6, C10, C13, S2, S4–S6). (**C, right**) Primary human myoblast differentiation into myotubes under treatment with simvastatin and/or fatty acids. Myotube fusion index was determined by counting MYHI (red) positively immunolabelled myotubes and HOECHST (blue) stained nuclei using the cell image analysis software CellProfiler v.2.1.1. Error/bars represent mean with SD. (95% confidence interval; right side – positive effect, left side – negative effect; n = 8, cell populations C5, C6, C10, C13, S2–S6, 2-4 immunofluorescent pictures counted each). (**D**) Primary human statin-treated myotubes regain normal morphology when AL-8810 is added to the medium. (cell populations C12, C13) See also Supplementary Fig. S5. For cell populations used see Supplementary Table S1. [UT, untreated (black); Sim, simvastatin (red); Rosu, rosuvastatin (blue); MYHI, myosin heavy chain 1].

into malonyl-CoA (Mal-CoA), the primary substrate for fatty acid biosynthesis. Mal-CoA inhibits CPT1 for ß-oxidations. On the other hand, Ac-CoA can be metabolised by ACC and fatty acid synthase via transformation of palmitic acid and various fatty acids into acyl-CoA for ß-oxidation. Active CPT1 shuttles acyl-CoA into the inner mitochondrial vortex for ß-oxidation[32]. In rodents, high CPT1 levels have been shown to induce mitochondrial overload by acyl-carnitine accumulation with excess ß-oxidation leading to insulin resistance[33] and mitochondrial stress[34]. High CPT1 values in statin-treated primary human myotubes may hint towards altered ß-oxidation and mitochondrial impairment. Insulin resistance under statin treatment would be interesting for further studies.

In the cytosol, fatty acid synthases, desaturases, and elongases synthesize long-chain fatty acids by using Mal-CoA and Ac-CoA. Fatty acid desaturases catalyse the formation of arachidonic acid and eicosapentanoic acid, the precursor of prostaglandins and eicosanoids. These molecules have multiple effects including influences on cell proliferation and differentiation[35], inflammation, mitochondrial function, and being pain mediators, a very frequent complaint of statin-users. The degree of statin influence on prostaglandin and eicosanoid synthesis was striking at molecular level, i.e. on fatty acid desaturases, elongases, de-/carboxylases (see Supplementary Table S8, Fig. 3A,B). We concentrated our further investigation on the formation of prostaglandins and eicosanoids. As the next important enzyme being significantly downregulated, PTGS1 (COX1) converts ω-6 derived arachidonic acid into biological active eicosanoids and prostaglandins, i.e. PGE2, PGD2, and PGF2a. PTGS is interesting because nonsteroidal anti-inflammatory drugs such as ibuprofen inhibit PTGS and are relevant for pain management[36]. PTGS-inhibitors influence on human skeletal muscle is controversially reported[35,37–39]. In older patients performing resistance exercise under PTGS-inhibition treatment, Type I fiber size increased up to 28% compared to control group[39]. Beneficial effects on skeletal muscle performance have been reported for PTGS up-regulation at mRNA level[40]. Decreased satellite cell fusion after PTGS1 inhibition has been observed in rats[41]. We found that PTGS1 expression is associated with reduced differentiation of simvastatin-treated primary human myotubes. PTGS1 is suggested as the only source for PGF2a[42] derived from arachidonic acid. PGF2a acts pro-inflammatory but at the same time suggested to promote murine myoblasts fusion <u>and</u> proliferation[43,44]. Its inhibition is proposed to significantly diminish murine myoblast fusion as reported by Horsely *et al.*[43]. Contrary to the data in animals, Brewer *et al.* found no significant effect in human skeletal muscle with PGF2a metabolite inhibition and any negative effect diminished over time[35]. In our study, treatment with PGF2a did not significantly change myoblast proliferation and differentiation under statin treatment but PGF2a secretion initially increased under simvastatin treatment together with PGD2, another proinflammatory PG. In a clinical study, eccentric resistance exercise initially revealed high PGF2a levels in human skeletal muscle biopsy specimens[45]. PGD2 metabolites are also linked to Duchenne Muscular Dystrophy (DMD) suggesting a role in muscle cell pathology[46]. Our findings support data obtained from human skeletal muscle[37] rather than from mice and rats[41,43]. Inflammation resolving metabolites derived from ω-6 arachidonic acid derived (lipoxins LXA4, LXB4), ω-3 docosahexaenoic acid (RvD2), and ω-3 eicosapentanoic acid (PGE3) were found secreted after statin treatment. A specific role for these metabolites in muscle cells is still unknown. For PGE3, anti-proliferative activities have been reported for tumour cells[47]. Peroxidation of ω-6 fatty acids via arachidonate 15-lipoxygenase produces 13-HODE. Its complete absence for simvastatin samples was surprising. Beside its activating capability for peroxisome proliferator-activated receptors and G protein coupled receptor, 13-HODE is speculated for mitochondria dysfunction and altered calcium homeostasis in epithelia cells[48]. There is currently no information for 13-HODE in skeletal muscle cells but may be another intriguing candidate to be studied in myoblast fusion. Taken together, lipid profiles from supernatant of statin-treated primary human muscle cells under fusion condition show increase in ω-6 arachidonic acid metabolites. However, supplements with ω-3 eicosapentanoic acid and docosahexaenoic acid, but not ω-6, are reported to improve skeletal muscle damage, stiffness and regeneration[49–51]. *In vivo* studies in elderly human probands and insulin-resistant non-diabetic patients, ω-3 PUFA supplementation had no effect on mitochondrial function[49,52] but improved mitochondrial ADP kinetics and insulin sensitivity in young, healthy adults[53]. Pre-treatment with ω-3 fatty acid eicosapentanoic acid but not docosahexaenoic acid stimulates fatty acid ß-oxidation and glucose transport in human myotubes[54]. Here, we showed that AL-8810, a PGF2a-receptor agonist[35], positively influences simvastatin-induced effects on muscle cell proliferation and differentiation. We speculate that AL-8810 quenches excess levels of PGF2a, initially secreted by simvastatin treated primary human myoblasts at a critical time point for fusion. We believe that our bench side findings could be translated into the clinic. The lower effect of rosuvastatin on the human muscle cells *in vitro* suggests that patients should be treated with rosuvastatin instead of simvastatin. However, muscular side effects have also been observed with rosuvastatin in clinic. Very recently, a clinical study showed that eicosapentanoic acid and docosahexaenoic acid reduced pain and stiffness as musculoskeletal symptoms in coronary artery disease patients[55] and was also shown to be safe in combination with statins[56]. Our study provides an explanation and supports the notion that ω-3 fatty acids should be added to statin therapy either as a prevention or as a treatment of statin myopathy. Patients may be less inclined to discontinue treatment when statin muscular side effects including pain are reduced.

Materials and Methods

Primary human myoblasts and cell populations. Muscle biopsy specimens for myoblast isolation were obtained from musculus vastus lateralis (M. vast. lat.) after Institutional Review Board (IRB) approval by the regulatory agencies (EA1/203/08 and EA2/051/10, Charité Universitätsmedizin Berlin, in compliance with the Declaration of Helsiniki) at the Helios Hospital Berlin Buch, Berlin, Germany, for diagnostic or orthopedic reasons. All study participants provided informed consent. Human muscle biopsy material is restricted regarding availability and quantity, also for ethical reasons. Experiments were conducted from a total of 22 different primary human myoblast cultures (Supplementary Table S1). All cells used in this study were maintained at 37 °C in 5% CO2. For all experiments, except for eicosanoid substitutions, we only used primary muscle cells

obtained from statin naïve individuals. Statin-myopathy patients had myalgias (>3 of 10 on a visual analogue scale) and/or creatine kinase levels elevated to >250 IU/l under therapy. Isolation was performed as described[57]. Briefly, muscle specimens were digested in Collagenase CLS II (Biochrom AG, Germany), 2.5 U/mL Dispase II (Roche, Germany), 0.03% Trypsin and 125 μM EDTA. Outgrowing cells were expanded in Skeletal Muscle Cell Growth Medium (ProVitro, Germany) and myoblasts were purified using anti-CD56 coated magnetic beads (Miltenyi Biotech, Germany). The percentage of fibroblasts in myoblast cultures was always below 5% as assessed by anti-desmin staining. Differentiation into myotubes was induced using Opti-MEM (Invitrogen, Germany).

We controlled for confounding factors including cell culture, sample handling, and biopsy-stress variations. At least two to a maximum of four cell populations were used simultaneously in an experimental setup by the same experimenter. In an experimental setup, controls and both statins were completed simultaneously.

Pharmacological reagents. The active form of simvastatin was purchased from ARC (Missouri, USA), rosuvastatin from LKT Laboratories (Minnesota, USA), fatty acid species from Cayman Chemical (Michigan, USA). Geranylgeranyl-pyrophosphate (GGP), mevalonolactone (MVAL), and mevalonic acid (MVA) were from Sigma Aldrich (Germany). Both statins were dissolved in DMSO and tested for their functionality at different concentrations (1–50 μM). (Supplementary Table S11).

Treatment of myoblast and myotubes. Primary human myoblasts were cultured in skeletal muscle growth medium (ProVitro, Berlin, Germany) in 96 well plates (3×10^3 cells/well). Test substances were applied 24 h after plating (Supplementary Table S11). Every 24 h, the cells were refed with fresh medium in the presence or absence of test compounds. All treatments were performed in parallel for each cell population at the same time of the day to exclude circadian rhythm effects. Proliferation was quantified by the colorimetric BrdU assay (Roche, Germany). Toxicity was assessed using the ToxiLight™ Non-destructive Cytotoxicity BioAssay Kit (Lonza, Cologne, Germany), and the Cytotoxicity Detection Kit (Roche, Germany). Amplex® Red Cholesterol Assay Kit (Invitrogen, Germany) was used to measure cholesterol. Mevalonate and cholesterol levels were determined under delipidated medium conditions. The cells were examined after 24 h, 48 h, 72 h, and 96 h. For differentiation into myotubes, primary human myoblasts at a 70% confluence were serum starved with Opti-MEM (Invitrogen, Germany). Selected eicosanoid species were added to myoblast cultures under proliferation and differentiation condition with and without statins. Statins were titrated to a concentration effective for both simvastatin and rosuvastatin using proliferation, toxicity, and mevalonate detection tests as measures. Eicosanoid concentrations were used as suggested by the literature. (Supplementary Table S11, Supplementary Fig. S2).

Mevalonic acid in statin-treated primary human myotubes. Together with Lipidomix GmbH (Berlin, Germany), we developed a new and easy method to detect mevalonate intracellular in primary human muscle cells. Cells were lysed by three freeze and thaw cycles and mechanically using 21, 23, and 26 Gauge needles [Lysis buffer: 20 mM Tris-HCl pH 7,4; 150 mM NaCl; 1 mM EDTA; 1 mM PMSF; 1 x Complete Protease-Inhibitor (Roche, Germany)]. Protein concentration was determined using BCA kit (Biorad, Germany). After lysis, proteins were precipitated with 1/10 volume 4 M HClO4 for 10–20 min at 4 °C. When pH was neutralised with 5 N KOH, samples were mixed and incubated with 1/5 volume 6 M HCl at 4 °C for at least 15 h to promote conversion of mevalonate into mevalonolactone. After centrifugation at 13,000 x g for 2 min, further analysis using HPLC/MS/MS was performed by Dr. Michael Rothe at Lipidomix GmbH, Berlin, Germany. Mevalonolactone HPLC/MS/MS measurements are described in the Supplementary Method section in more detail. (Supplementary Table S12, Supplementary Fig. S6).

RNA analyses. RNA was isolated using the NucleoSpin® RNA/Protein Kit (Marcherey-Nagel, Germany). RNA quantity and purity were determined using a NanoDrop ND-1000 spectrophotometer (Thermo Scientific, USA). For qPCR, the mRNA was reverse transcribed using the QuantiTect reverse transcription kit (Qiagen, Germany). qPCR was performed according to Minimum Information for Publication of Quantitative Real-Time PCR Experiments (MIQE) guidelines[58] using SYBR Green I in the Mx3000P instrument (Stratagene, Germany) (Primer sequences in Supplementary Table S4) with two to three reference genes. C_T-value replicates were checked for consistency and PCR primer efficacy (%) was determined.

RNA sequencing. RNA quality was determined using Agilent 2100 bioanalyzer (Agilent Technologies, USA). The RIN factor was > 8 for all samples. cDNA libraries for paired-end sequencing were prepared using the TruSeq Stranded mRNA library preparation kit (Illumina, USA). RNA sequencing was performed at Illumina HiSeq platform (Illumina, USA).

Pre-processed raw RNA-Seq data were imported into CLC Genomics Workbench (v. 7.5.1) and processed using a standardized workflow. The workflow defines the following steps: (1) trimming sequences (2) creating sequence quality check report (3) RNA-Seq analysis with reporting of read tracks, gene expression tracks, transcript expression tracks, fusion tracks, and un-mapped reads. All samples passed the RNA-seq quality check (Supplementary Fig. S1). Trimmed reads were aligned to human reference genome (GRCh37) and mapped back to the human transcriptome (v. 19). Mapped read counts were statistically analyzed using the R packages EdgeR and DESeq for matched sample data[59]. Samples without any and with DMSO treatment were considered as reference group. Gene expression data from simvastatin and rosuvastatin treated samples with FDR < 0.05 were considered as statistically significantly different from control groups. Data are stored at Gene Expression Omnibus - GSE107998.

Transcriptional profiling can be influenced by unintentional factors. We controlled for confounding factors including individual differences, muscle biopsy variations, and sample composition. The muscle cell population were obtained from age-matched donors from the same ethnic group during an orthopaedic surgery. Gender specific genes were removed for RNAseq statistic. qPCR analyses verified RNAseq expression results of selected candidate genes.

Deep proteome analysis. Proteins were prepared according to Sapcariu et al.[60]. Samples were measured by LC-MS/MS on a Q-Exactive orbitrap mass spectrometer (Thermo Scientific, Germany). For the data analysis, the MaxQuant software package version 1.4.1.2 was used, with a multiplicity of 3 for dimethylation analysis (modified epsilon amino groups of lysine plus modified N-terminal amino groups)[61]. Carbamidomethylation was set as a fixed modification while oxidized methionine and acetylated N-termini were set as variable modifications. The method is described in more detail in the Supplementary Method section. An FDR of 0.01 was applied for peptides and proteins search was performed using a human Uniprot database (August 2013). Normalized ratios of the protein groups output were used to determine proteins which are obviously regulated. (Supplementary Fig. S1).

Cell quantification. Myotube fusion and maturation were quantified using an LSM 700 AxioObserver Z1 (Zeiss, Germany) and an N-Achroplan 10 × /0.25 M27 or 40x objective. LSM image files were analysed with ZEN 2012 (Zeiss, Germany) and exported. Immunofluorescence images in Figs. 4, S4 and S5 are representative data and the ZEN 2012 software option "Best Fit" was applied for all images before exporting into bitmap files. For cell quantification, image files were converted in batch into black-white images with adjusted gray-scale using IrfanView (v.4.38). Separate image files for MYHCf and HOECHST 33258 were loaded into the CellProfiler software (v 2.1.1)[62,63]. A pipeline for calculating multinucleated cells was used and slightly modified[64]. A myotube was defined having more than three nuclei. The fusion index was calculated by the number of nuclei in myotubes divided by the total number of nuclei counted in each image. The maturation index is described by the average number of nuclei per myotube.

Data visualization for RNA-Seq and deep proteome. For analyses with mapped count data apart from the EdgeR or DESeq package, mapped read counts were exported from CLC Genomics Workbench (v 7.5.1) and normalized for their library size using the trimmed mean of M-values normalization approach (TMM)[65]. Differential gene expression data were plotted as dendogram clustered heatmaps using GENE-E (v 3.0.206)[66]. Plot.ly was used to visualize quality check data. Principal component analysis was performed in discriminate gene expression data for each treatment group with ClustVis (release June 2016)[67]. Venny 2.0 was used to generate the Venn diagram[68]. The Circos-Plot for omics data was generated using the Bioconductor package OmicCircos[69].

Pathway analyses. Statistically significant, differential gene expression data from simvastatin and rosuvastatin treated myotubes and controls were further analysed with GOrilla (release March 2013), Reactome (v 53), and DAVID (v 6.7) to identify enriched gene ontology (GO) terms and pathway clustering[70–72]. Gene lists were ranked regarding their expression value. In addition, the web-based Ingenuity pathway analysis application (IPA; Ingenuity Systems, Redwood City, CA) was used.

Statistics. All statistics for RNA-Seq and proteome data analyses were performed using RStudio (v 0.98.1006) for executing R packages (v 3.1.1). Statistical analyses for proliferation, toxicity, and qPCR data were performed with GraphPad Prism (v 8.0) using the One-way ANOVA corrected with Holm-Sidak/Dunn's method. Two-way ANOVA for multiple testing was used for all data obtained from statin, rescue experiments, and fatty acid species treated primary human muscle cells. Each comparison stands for its own. Data obtained from western blots with protein from primary human myotubes were analysed for statistical significance using two-tailed Mann-Whitney test. Values of p are shown by asterisks using the standard convention: *$p \leq 0.05$; **$p \leq 0.01$; ***$p \leq 0.001$; ****$p \leq 0.0001$.

Data availability

All primary data are available upon science-based request.

Bulk RNAseq data are available at NCBI GEO accession: GSE107998.
https://www.ncbi.nlm.nih.gov/geo/query/acc.cgi?acc=GSE107998

References

1. Cohen, J. D., Brinton, E. A., Ito, M. K. & Jacobson, T. A. Understanding Statin Use in America and Gaps in Patient Education (USAGE): an internet-based survey of 10,138 current and former statin users. *J. Clin. Lipidol.* **6**, 208–15 (2012).
2. Collins, R. *et al.* Interpretation of the evidence for the efficacy and safety of statin therapy. *Lancet* **388**, 2532–2561 (2016).
3. Jacobson, T. A. *et al.* The STatin Adverse Treatment Experience Survey: Experience of patients reporting side effects of statin therapy. *J. Clin. Lipidol.* **13**, 415–424 (2019).
4. Kaiser, C. Statin Side Effects Stymie Compliance | MedPage Today. (2012). Available at, https://www.medpagetoday.org/cardiology/dyslipidemia/33422?vpass=1. (Accessed: 31st July 2017).
5. Deedwania, P. & Lardizabal, P. C. Benefits of statin therapy and compliance in high risk cardiovascular patients. *Vasc. Health Risk Manag.* **6**, 843 (2010).
6. Newman, C. B. *et al.* Statin Safety and Associated Adverse Events: A Scientific Statement From the American Heart Association. *Arterioscler. Thromb. Vasc. Biol.* **39** (2019).
7. Pedro-Botet, J., Climent, E. & Benaiges, D. Muscle and statins: from toxicity to the nocebo effect. *Expert Opin. Drug Saf.* **18**, 573–579 (2019).
8. Zhang, P., Verity, M. A. & Reue, K. Lipin-1 Regulates Autophagy Clearance and Intersects with Statin Drug Effects in Skeletal Muscle. *Cell Metab.* **20**, 267–279 (2014).
9. Koren, M. J. *et al.* Long-Term Efficacy and Safety of Evolocumab in Patients With Hypercholesterolemia. *J. Am. Coll. Cardiol.* **74**, 2132–2146 (2019).
10. Knoblauch, H., Schoewel, V., Kress, W., Rosada, A. & Spuler, S. Another Side to Statin-Related Side Effects. *Ann. Intern. Med.* **152**, 478 (2010).
11. Thompson, P. D., Panza, G., Zaleski, A. & Taylor, B. Statin-Associated Side Effects. *J. Am. Coll. Cardiol.* **67**, 2395–2410 (2016).

12. Tamanoi, F., Azizian, M., Ashrafi, M. & Bathaie, S. Mevalonate Pathway and Human Cancers. *Curr. Mol. Pharmacol.* **10**, 77–85 (2017).
13. Bookstaver, D. A., Burkhalter, N. A. & Hatzigeorgiou, C. Effect of coenzyme Q10 supplementation on statin-induced myalgias. *Am. J. Cardiol.* **110**, 526–9 (2012).
14. Gupta, A. & Thompson, P. D. The relationship of vitamin D deficiency to statin myopathy. *Atherosclerosis* **215**, 23–29 (2011).
15. Pennisi, M. *et al.* Vitamin D Serum Levels in Patients with Statin-Induced Musculoskeletal Pain. *Dis. Markers* **2019**, 1–6 (2019).
16. Qu, H. *et al.* The effect of statin treatment on circulating coenzyme Q10 concentrations: an updated meta-analysis of randomized controlled trials. *Eur. J. Med. Res.* **23**, 57 (2018).
17. Farooqi, M. A. M. *et al.* Statin therapy in the treatment of active cancer: A systematic review and meta-analysis of randomized controlled trials. *PLoS One* **13**, e0209486 (2018).
18. Martín Sánchez, C. *et al.* Disruption of the mevalonate pathway induces dNTP depletion and DNA damage. *Biochim. Biophys. Acta - Mol. Cell Biol. Lipids* **1851**, 1240–1253 (2015).
19. Schirris, T. J. J. *et al.* Statin-Induced Myopathy Is Associated with Mitochondrial Complex III Inhibition. *Cell Metab.* **22**, 399–407 (2015).
20. Reinhart, K. M. & Woods, J. A. Strategies to preserve the use of statins in patients with previous muscular adverse effects. *Am. J. Heal. Pharm.* **69**, 291–300 (2012).
21. Grunwald, S. A. *et al.* A prostaglandin alpha F2 analog protects from statin-induced myopathic changes in primary human muscle cells. *bioRxiv* 271932, https://doi.org/10.1101/271932 (2019).
22. Schwanhäusser, B. *et al.* Global quantification of mammalian gene expression control. *Nature* **473**, 337–342 (2011).
23. Medina, M. W. & Krauss, R. M. The Role of HMGCR Alternative Splicing in Statin Efficacy. *Trends Cardiovasc. Med.* **19**, 173–177 (2009).
24. Leszczynska, A. *et al.* Different statins produce highly divergent changes in gene expression profiles of human hepatoma cells: a pilot study. *Acta Biochim. Pol.* **58**, 635–9 (2011).
25. Wang, H. H., Garruti, G., Liu, M., Portincasa, P. & Wang, D. Q.-H. Cholesterol and Lipoprotein Metabolism and Atherosclerosis: Recent Advances in Reverse Cholesterol Transport. *Ann. Hepatol.* **16**, S27–S42 (2017).
26. Boschmann, M. *et al.* Dipeptidyl-Peptidase-IV Inhibition Augments Postprandial Lipid Mobilization and Oxidation in Type 2 Diabetic Patients. *J. Clin. Endocrinol. Metab.* **94**, 846–852 (2009).
27. Burg, J. S. & Espenshade, P. J. Regulation of HMG-CoA reductase in mammals and yeast. *Prog. Lipid Res.* **50**, 403–410 (2011).
28. Cooney, C. A. Drugs and supplements that may slow aging of the epigenome. *Drug Discov. Today Ther. Strateg.* **7**, 57–64 (2010).
29. Perry, R. J. *et al.* Hepatic Acetyl CoA Links Adipose Tissue Inflammation to Hepatic Insulin Resistance and Type 2 Diabetes. *Cell* **160**, 745–758 (2015).
30. Betteridge, D. J. & Carmena, R. The diabetogenic action of statins - mechanisms and clinical implications. *Nat. Rev. Endocrinol.* **12**, 99–110 (2016).
31. Margerie, D. *et al.* Hepatic transcriptomic signatures of statin treatment are associated with impaired glucose homeostasis in severely obese patients. *BMC Med. Genomics* **12**, 80 (2019).
32. Wakil, S. J. & Abu-Elheiga, L. A. Fatty acid metabolism: target for metabolic syndrome. *J. Lipid Res.* **50**, S138–S143 (2009).
33. Koves, T. R. *et al.* Mitochondrial Overload and Incomplete Fatty Acid Oxidation Contribute to Skeletal Muscle Insulin Resistance. *Cell Metab.* **7**, 45–56 (2008).
34. Ly, L. D. *et al.* Oxidative stress and calcium dysregulation by palmitate in type 2 diabetes. *Exp. Mol. Med.* **49**, e291 (2017).
35. Jansen, K. M. & Pavlath, G. K. Prostaglandin F2alpha promotes muscle cell survival and growth through upregulation of the inhibitor of apoptosis protein BRUCE. *Cell Death Differ.* **15**, 1619–28 (2008).
36. Grösch, S., Niederberger, E. & Geisslinger, G. Investigational drugs targeting the prostaglandin E2 signaling pathway for the treatment of inflammatory pain. *Expert Opin. Investig. Drugs* **26**, 51–61 (2017).
37. Brewer, C. B., Bentley, J. P., Day, L. B. & Waddell, D. E. Resistance exercise and naproxen sodium: effects on a stable PGF2α metabolite and morphological adaptations of the upper body appendicular skeleton. *Inflammopharmacology* **23**, 319–327 (2015).
38. Trappe, T. A. *et al.* Influence of acetaminophen and ibuprofen on skeletal muscle adaptations to resistance exercise in older adults. *Am. J. Physiol. Integr. Comp. Physiol.* **300**, R655–R662 (2011).
39. Trappe, T. A. *et al.* COX Inhibitor Influence on Skeletal Muscle Fiber Size and Metabolic Adaptations to Resistance Exercise in Older Adults. *J. Gerontol. A. Biol. Sci. Med. Sci.* **71**, 1289–94 (2016).
40. Mansueto, G. *et al.* Transcription Factor EB Controls Metabolic Flexibility during Exercise. *Cell Metab.* **25**, 182–196 (2017).
41. Mendias, C. L., Tatsumi, R. & Allen, R. E. Role of cyclooxygenase-1 and -2 in satellite cell proliferation, differentiation, and fusion. *Muscle Nerve* **30**, 497–500 (2004).
42. Liu, S. Z. *et al.* Prostaglandin E 2/cyclooxygenase pathway in human skeletal muscle: influence of muscle fiber type and age. *J. Appl. Physiol.* **120**, 546–551 (2016).
43. Horsley, V. & Pavlath, G. K. Prostaglandin F 2α stimulates growth of skeletal muscle cells via an NFATC2-dependent pathway. *J. Cell Biol.* **161**, 111–118 (2003).
44. Yew, S. F., Reeves, K. A. & Woodward, B. Effects of prostaglandin F2 alpha on intracellular pH, intracellular calcium, cell shortening and L-type calcium currents in rat myocytes. *Cardiovasc. Res.* **40**, 538–45 (1998).
45. Trappe, T. A., Fluckey, J. D., White, F., Lambert, C. P. & Evans, W. J. Skeletal muscle PGF(2)(alpha) and PGE(2) in response to eccentric resistance exercise: influence of ibuprofen acetaminophen. *J. Clin. Endocrinol. Metab.* **86**, 5067–70 (2001).
46. Nakagawa, T. *et al.* A prostaglandin D2 metabolite is elevated in the urine of Duchenne muscular dystrophy patients and increases further from 8years old. *Clin. Chim. Acta* **423**, 10–14 (2013).
47. Fan, Y.-Y., Davidson, L. A., Callaway, E. S., Goldsby, J. S. & Chapkin, R. S. Differential effects of 2- and 3-series E-prostaglandins on *in vitro* expansion of Lgr5+ colonic stem cells. *Carcinogenesis* **35**, 606–12 (2014).
48. Mabalirajan, U. *et al.* 12/15-lipoxygenase expressed in non-epithelial cells causes airway epithelial injury in asthma. *Sci. Rep.* **3**, 1540 (2013).
49. Lalia, A. Z. *et al.* Effects of Dietary n-3 Fatty Acids on Hepatic and Peripheral Insulin Sensitivity in Insulin-Resistant Humans. *Diabetes Care* **38**, 1228–1237 (2015).
50. Ochi, E., Tsuchiya, Y. & Yanagimoto, K. Effect of eicosapentaenoic acids-rich fish oil supplementation on motor nerve function after eccentric contractions. *J. Int. Soc. Sports Nutr.* **14**, 23 (2017).
51. Tsuchiya, Y., Yanagimoto, K., Ueda, H. & Ochi, E. Supplementation of eicosapentaenoic acid-rich fish oil attenuates muscle stiffness after eccentric contractions of human elbow flexors. *J. Int. Soc. Sports Nutr.* **16**, 19 (2019).
52. Lalia, A. Z. *et al.* Influence of omega-3 fatty acids on skeletal muscle protein metabolism and mitochondrial bioenergetics in older adults. *Aging (Albany. NY).* **9**, 1096–1129 (2017).
53. Herbst, E. A. F. *et al.* Omega-3 supplementation alters mitochondrial membrane composition and respiration kinetics in human skeletal muscle. *J. Physiol.* **592**, 1341–1352 (2014).
54. Løvsletten, N. G. *et al.* Increased triacylglycerol - Fatty acid substrate cycling in human skeletal muscle cells exposed to eicosapentaenoic acid. *PLoS One* **13**, e0208048 (2018).
55. Alfaddagh, A. *et al.* The effect of eicosapentaenoic and docosahexaenoic acids on physical function, exercise, and joint replacement in patients with coronary artery disease: A secondary analysis of a randomized clinical trial. *J. Clin. Lipidol.* **12**, 937–947.e2 (2018).

56. Alfaddagh, A. *et al*. Effect of Eicosapentaenoic and Docosahexaenoic Acids Added to Statin Therapy on Coronary Artery Plaque in Patients With Coronary Artery Disease: A Randomized Clinical Trial. *J. Am. Heart Assoc.* **6** (2017).
57. Marg, A. *et al*. Sarcolemmal repair is a slow process and includes EHD2. *Traffic* **13**, 1286–94 (2012).
58. Bustin, S. A. *et al*. The MIQE Guidelines: Minimum Information for Publication of Quantitative Real-Time PCR Experiments. *Clin. Chem.* **55**, 611–622 (2009).
59. Lohse, M. *et al*. RobiNA: a user-friendly, integrated software solution for RNA-Seq-based transcriptomics. *Nucleic Acids Res.* **40**, W622–7 (2012).
60. Sapcariu, S. C. *et al*. Simultaneous extraction of proteins and metabolites from cells in culture. *MethodsX* **1**, 74–80 (2014).
61. Cox, J. & Mann, M. MaxQuant enables high peptide identification rates, individualized p.p.b.-range mass accuracies and proteome-wide protein quantification. *Nat. Biotechnol.* **26**, 1367–1372 (2008).
62. Bray, M.-A., Vokes, M. S. & Carpenter, A. E. Using CellProfiler for Automatic Identification and Measurement of Biological Objects in Images. in Current Protocols in Molecular Biology 109, 14.17.1–14.17.13 (John Wiley & Sons, Inc., 2015).
63. Carpenter, A. E. *et al*. CellProfiler: image analysis software for identifying and quantifying cell phenotypes. *Genome Biol.* **7**, R100 (2006).
64. Logan, D. Calculating multinucleated cells in muscle fibers - Image Analysis - Image.sc Forum. Available at, https://forum.image.sc/t/calculating-multinucleated-cells-in-muscle-fibers/12776/2 (2014).
65. Robinson, M. D., McCarthy, D. J. & Smyth, G. K. edgeR: a Bioconductor package for differential expression analysis of digital gene expression data. *Bioinformatics* **26**, 139–140 (2010).
66. Gould, J. GENE-E. Available at, https://software.broadinstitute.org/GENE-E/index.html (2016).
67. Metsalu, T. & Vilo, J. ClustVis: a web tool for visualizing clustering of multivariate data using Principal Component Analysis and heatmap. *Nucleic Acids Res.* **43**, W566–70 (2015).
68. Oliveros, J. C. Venny. An interactive tool for comparing lists with Venn's diagrams. Available at, https://bioinfogp.cnb.csic.es/tools/venny/index.html (2015).
69. Hu, Y. *et al*. OmicCircos: A Simple-to-Use R Package for the Circular Visualization of Multidimensional Omics Data. *Cancer Inform.* **13**, 13–20 (2014).
70. Dennis, G. *et al*. DAVID: Database for Annotation, Visualization, and Integrated Discovery. *Genome Biol.* 4, (P3 (2003).
71. Eden, E., Navon, R., Steinfeld, I., Lipson, D. & Yakhini, Z. GOrilla: a tool for discovery and visualization of enriched GO terms in ranked gene lists. *BMC Bioinformatics* **10**, 48 (2009).
72. Vastrik, I. *et al*. Reactome: a knowledge base of biologic pathways and processes. *Genome Biol.* **8**, R39 (2007).

Acknowledgements

Author contributions

S.A.G, O.P., S.H., N.J., K.S., G.P., G.D. performed experiments and analysed data. U.G., E.S.-T. recruited patients. W.K. performed genetic analysis. S.A.G., E.S.-T., S.S. designed and organized the study and analysed data. S.A.G. and S.S. wrote the manuscript.

Competing interests

The authors declare no competing interests.

Additional information

Supplementary information is available for this paper at https://doi.org/10.1038/s41598-020-58668-2.

Correspondence and requests for materials should be addressed to S.A.G. or S.S.

Reprints and permissions information is available at www.nature.com/reprints.

Publisher's note Springer Nature remains neutral with regard to jurisdictional claims in published maps and institutional affiliations.